Adsorption of Nanoceria by Phosphocholine Liposomes

Yibo Liu and Juewen Liu*

Department of Chemistry, Waterloo Institute for Nanotechnology, University of Waterloo,

Waterloo, Ontario, N2L 3G1, Canada

Email: liujw@uwaterloo.ca

Abstract

Nanoceria (CeO_2 nanoparticle) possesses a number of enzyme-like activities. In particular, it scavenges reactive oxygen species (ROS) leading in vitro and in vivo anti-oxidation studies. An important aspect of fundamental physical understanding is its interaction with lipid membranes, the man component of the cell membrane. In this work, adsorption of nanoceria onto phosphocholine (PC) liposomes was performed. PC lipids are the main constituent of the cell outer membrane. Using fluorescence quenching assay, nanoceria adsorption isotherm was determined at various pH's and ionic strengths. A non-Langmuir isotherm occurred at pH 4.0 due to lateral electrostatic repulsion among adsorbed cationic nanoceria. The phosphate group in the PC lipid is mainly responsible for the interaction, and adsorbed nanoceria can be displaced by free inorganic phosphate. The tendency of the system to form large aggregates is a function of pH and the concentration of nanoceria, attributable to nanoceria being positively charged at pH 4 and neural at physiological pH. Calcein leakage test indicates that nanoceria induces liposome leakage due to transient lipid phase transition, and cryo-TEM indicates that the overall shape of the liposome is retained although deformation is still observed. This study provides fundamental biointerfacial information at a molecular level regarding the interaction of nanoceria and model cell membranes.

Introduction

CeO_2 nanoparticles (NP) or nanoceria are an important material as catalysts, gas sensors, UV filters, and solid oxide fuel cells.[1] Its unique properties are attributed to the surface Ce^{3+} ions, providing a redox couple with Ce^{4+}.[2, 3] The Ce^{3+} sites are accompanied by oxygen vacancies near the surface. Therefore, small CeO_2 NPs of several nanometers possess enhanced activities due to a large surface-to-volume ratio.[4-6]

With high biocompatibility, nanoceria is also an attractive material for various biological applications.[2, 4] For example, it was reported that nanoceria can scavenge reactive oxygen species (ROS) in living systems with superoxide dismutase and catalase-like activities.[2, 7-9] In a few cases, nanoceria protected cells from oxidative stress induced by ROS or radiation.[10-14] It was also reported that nanoceria protects normal cells but not cancer cells.[15] On the other hand, CeO_2 nanorods with a high aspect ratio had pro-inflammatory effects.[16] In vivo studies revealed that nanoceria fights against inflammation, ischemic stroke and radiation-induced damages.[11, 17] With so many biological applications, however, few studies touched upon its interaction with biological molecules,[18] especially biomembranes.[10, 16]

To enter cells, nanoceria has to first cross the cell membrane. Therefore, it is important to study its interaction with membranes.[19-21] The main components of the cell membrane are lipids with phosphocholine (PC) lipids being the most abundant on the outer membrane of eukaryotic cells. The interactions of PC membranes with various nanomaterials have been studied,[21-26] in particular, with various oxides.[27-30] A primary example is the spontaneous fusion of PC liposomes onto silica forming supported bilayers using van der Waals force.[31-33] In contrast, PC liposomes adsorb onto TiO_2 NPs via a stronger force, likely bonding with the lipid phosphate group.[27-29, 34, 35] Most of the metal oxide NPs studied so far have a size of several tens of

nanometer or larger. Compared to them, an interesting feature of nanoceria is its small size, which may exert a different behavior. For example, very small silica NPs behave completely different when mixed with PC liposomes compared to the larger ones.[36] While larger nanoceria can also be made, small particles (below 10 nm) are required for catalytic activity and biomedical relevance.[4-6] In this work, we explore the interaction between nanoceria of ~5 nm and PC liposomes in terms of adsorption, stability, and membrane integrity.

Materials and Methods

Chemicals. All the phospholipids were purchased from Avanti Polar Lipids (Alabaster, AL). CeO_2 dispersion (catalog number: 289744, 20 % dispersed in 2.5 % acetic acid), disodium calcein, and Triton X-100 were from Sigma Aldrich. 4-(2-hydroxyetyl)-1-piperazineethanesulfonic acid (HEPES), acetate, phosphate and sodium chloride were from Mandel Scientific (Guelph, ON, Canada). Milli-Q water was used to prepared all the buffers and suspensions.

Preparation of liposomes. Liposomes were prepared using the standard extrusion method through a 100 nm membrane as described previously.[27] DOPC (1,2-dioleoyl-*sn*-glycero-3-phosphocholine) and DPPC (1,2-dipalmitoyl-*sn*-glycero-3-phosphocholine) with a total mass of 2.5 mg were respectively dissolved in chloroform. For Rh (rhodamine)-labeled liposome, 1% Rh-PE (2-dioleoyl-sn-glycero-3-phosphoethanolamine-N-(lissaminerhodamine B sulfonyl) (ammonium salt) was included. After evaporating chloroform, the dried lipid films were stored at -20 °C under a N_2 atmosphere prior to use. To prepare liposomes, the lipid films were hydrated with 0.5 mL buffer (10 mM HEPES, 100 mM NaCl, pH 7.6) to reach a lipid concentration of 5 mg mL^{-1}. For DPPC liposome, the lipids films were hydrated at 60 °C for 2 h and were extruded at 60 °C. To encapsulate calcein, the lipid films were hydrated with 100 mM calcein overnight

followed by extrusion for 21 times. Free calcein was removed by passing 35 μL of the samples through a PD-10 column using 25 mM HEPES for elution. The first 600 μL of the fluorescent fraction was collected.

ζ-potential and dynamic light scattering (DLS). The ζ-potential of CeO_2 NPs (100 μg mL^{-1}) was measured at various pH's in water on a Malvern Zetasizer NanoZS90 with a He-Ne laser (633 nm) at 90° collecting optics. HCl and NaOH were used to adjust pH. The size was measured with CeO_2 (1 mg mL^{-1}, in 25 mM acetate buffer, pH 4) and with DOPC liposomes (100 μg mL^{-1} in 25 mM HEPES buffer, pH 7.6).

Liposome adsorption studied by fluorescence quenching. A CeO_2 suspension was gradually titrated into the Rh-liposome (50 μg mL^{-1}, 1 mL) in buffer (25 mM acetate, pH 4, or 25 mM acetate with 150 mM NaCl, or 25 mM HEPES, pH 7.6). CeO_2 stock solutions (1 or 10 mg mL^{-1}) were used for this titration. The fluorescence spectra were recorded using a Varian Eclipse fluorometer (Ex: 560 nm; Em: 592 nm).

Phosphate inhibition studies. CeO_2 NPs (10 mg mL^{-1}) were first incubated in phosphate buffer (100 mM) for 30 min to cap the surface with phosphate. Then, 5 or 10 μL above mixture was added to Rh-labeled liposomes (25 μg mL^{-1}, 1 mL) and the fluorescence was measured. To study displacement, to 1 mL Rh-labeled liposome (25 μg mL^{-1}), CeO_2 NPs were added. Afterwards, 20 μL phosphate buffer (500 mM, pH 7.6 or pH 4) was added and the fluorescence was measured.

Complex stability test. To a Rh-labeled liposome (50 μg mL^{-1}, 200 μL) in buffer (25 mM acetate, pH 4 or 25 mM HEPES, pH 7.6), a small amount of CeO_2 was added to reach a final concentration of 1, 2, 5, 10, 25, 50, 100, or 200 μg mL^{-1}. After 30 min incubation, the mixture was centrifuged at 10,000 rpm for 10 min to collect the supernatant. The supernatant was diluted

10 times and its fluorescence was measured. To re-disperse the DOPC/CeO_2, the complex was prepared in HEPES buffer (25 mM, pH 7.6) as above and centrifuged at 10,000 rpm for 10 min. The pellets were collected and re-dispersed in 200 μL acetate buffer (50 mM, pH 4). After sonication, the suspension was again centrifuged, the supernatant was collected and diluted 10 times for fluorescence measurement. In another case, the complexes were prepared in acetate buffer (25 mM, pH 4). After 30 min incubation, 150 mM NaCl was added to destabilize the DOPC/CeO_2 complexes. After centrifugation at 10,000 rpm for 10 min, the pellets were collected and re-dispersed in 200 μL HEPES (50 mM, pH 7.6) by sonication. These sample were again centrifuged at 10,000 rpm for 10 min, the supernatant was collected and diluted 10 times for fluorescence measurement.

Liposome leakage studies. To monitor CeO_2 NP induced liposome leakage, 3 μL of the above purified calcein-loaded liposomes were added to 597 μL HEPES buffer (25 mM, pH 7.6) in a quartz cuvette at room temperature. The background fluorescence was monitored for 5 min before adding various amount of CeO_2 NPs (e.g. 10 or 20 μL of 1 mg mL^{-1} CeO_2, or 5 μL of 10 mg mL^{-1} CeO_2). The fluorescence was monitored for another 20 min followed by adding 20 μL phosphate buffer (500 mM, pH 7.6). At 25 min, 10 μL of 5% Triton X-100 was added. Calcein was excited at 485 nm, and the emission was monitored at 525 nm.

Transmission electron microscopy (TEM) and Cryo-TEM. TEM measurements were performed on a Philips CM10 transmission electron microscope. A 10 μL CeO_2 solution was spotted on a 230 mesh holy carbon copper grid and extra solution on the grid was removed by filter paper. The sample was dried in air before measurement. Cryo-TEM sample was prepared by mixing DOPC liposomes (50 μg mL^{-1}) and CeO_2 (50 μg mL^{-1}) in acetate buffer (25 mM, pH 4). A 5 μL sample was spotted on a plasma treated carbon coated copper TEM grid. The gird was

blotted with two pieces of filter paper for 2 sec and quickly plunged into liquid ethane. The sample was then loaded to a liquid N_2 cooled cold stage imaged with a 200 kV field emission TEM (FEI Tecnai G2 F20) at -175 °C.

Differential scanning calorimetry (DSC). To measure the phase transition temperature (T_c), DPPC liposomes (100 μg mL^{-1}) and DPPC/CeO_2 (mass ratio of 1:1 and 1:5) were used. The samples were degassed prior to injection into the DSC sample cell, while the reference cell was filled with the corresponding buffer. Each sample was scanned from 25 to 65 °C with a rate of 1 °C min^{-1} using a VP-DSC instrument (MicroCal). Six scans were carried out for each sample and the fifth scan was plotted.

Results and Discussion

Characterization of nanoceria and liposomes. DLS characterization based on scattering intensity shows our CeO_2 NPs have an average hydrodynamic size of 20 nm, while the number-based size distribution is centered at ~5 nm (Figure 1a). It is known that light scattering strongly favors larger particles, and our data suggest that this nanoceria sample is slightly aggregated. Although many previous work prepared nanoceria capped by various ligands and polymers to facilitate dispersion,[14, 37, 38] we are interested in understanding the native surface property. As a result, our nanoceria did not have a strong capping ligand, explaining the moderate aggregation. A TEM micrograph shows the size of individual nanoceria is below 5 nm and some aggregates can be also observed (Figure 1a inset), which is consistent with the DLS data. Its crystallinity was confirmed by high-resolution TEM (HRTEM) (Figure 1b). Such small particles were used to ensure high catalytic activity.[4-6]

Next, we studied the surface charge of nanoceria with a careful pH titration. At pH lower than 7, nanoceria is positively charged, while the surface becomes negative at higher pH (Figure 1c). Therefore, at physiological pH, nanoceria is nearly charge neutral, which may affect its colloidal stability due to a lack of charge stabilization.

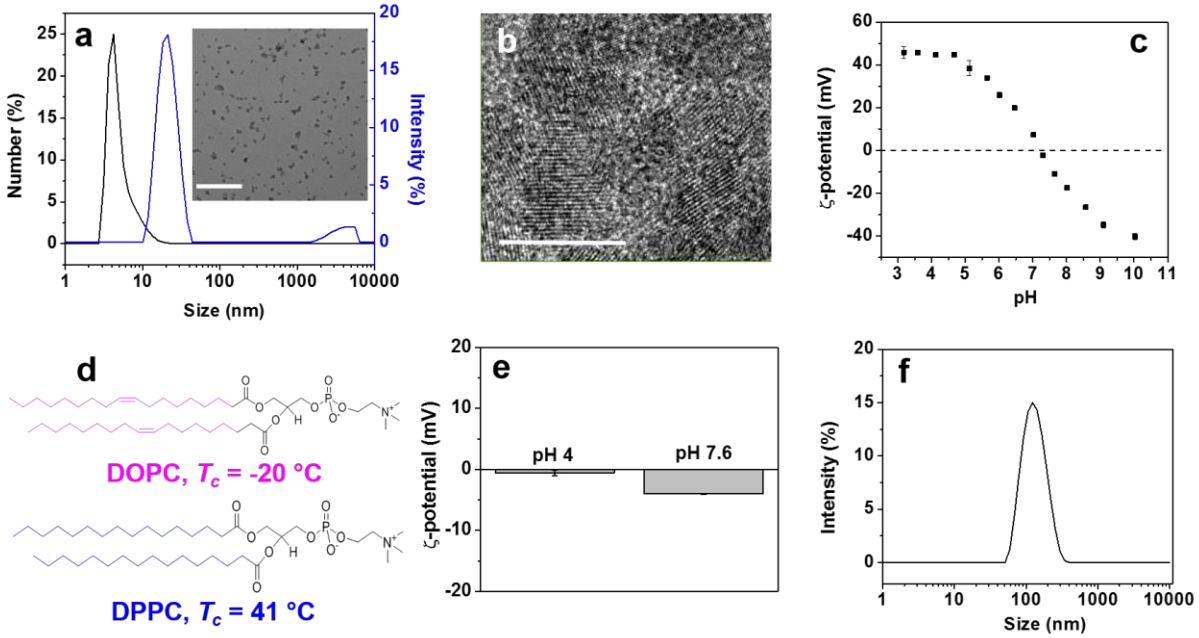

Figure 1. (a) DLS spectra of CeO_2 NPs dispersed in 25 mM acetate (pH 4) with both number and scattering intensity based distribution. Inset: a TEM micrograph of the sample (scale bar: 100 nm). (b) A HRTEM micrograph of CeO_2 NPs showing its crystalline structure (scale bar: 10 nm). (c) ζ-potential of CeO_2 NPs as a function of pH. (d) The structures of DOPC and DPPC lipids, and their phase transition temperature (T_c) values are labeled. (e) ζ-potential of DOPC liposomes in 25 mM acetate (pH 4) and HEPES (pH 7.6) buffers. (f) DLS spectrum of the DOPC liposomes in 25 mM HEPES (pH 7.6).

The structure of a DOPC lipid is shown in Figure 1d. Its headgroup contains a negatively charged phosphate and a positively charged choline. Therefore, this zwitterionic PC lipid is overall charge neutral, which is confirmed by ζ-potential measurement (Figure 1e). The neutral charge avoids electrostatic interactions with nanoceria. Based on our previous studies, the lipid phosphate group is likely to be important for interaction with nanoceria.[27-30] Our liposomes were prepared using the standard extrusion method through 100 nm pores, which is consistent with the DLS measurement of ~120 nm (Figure 1f).

Nanoceria is adsorbed by DOPC liposomes. To study their interaction, we first measured nanoceria adsorption by DOPC liposomes containing 1% rhodamine (Rh) label. To this liposome sample, we gradually titrated CeO_2 NPs at pH 4 and pH 7.6, respectively. We chose these two pH values since the catalytic activity of CeO_2 is the highest at pH 4,[39] while pH 7.6 is the physiological condition.

The fluorescence spectra of the Rh-labeled DOPC liposomes at different nanoceria concentrations are shown in Figure 2a, and an overall trend of fluorescence decrease is observed. We measured the UV-Vis spectra of our nanoceria and its mixture with DOPC liposome at pH 4 (Figure S1a), where no light scattering feature was observed. In addition, no light absorption was observed beyond 400 nm. Therefore, the drop of fluorescence cannot be explained by light scattering or the inner-filter effect. Nanoceria is a strong quencher for many adsorbed fluorophores.[40] Without light scattering, we attribute the fluorescence drop here to the adsorption of nanoceria by the liposome, directly quenching the associated Rh fluorophore.

The amount of quenching was quantified by plotting the relative fluorescence change ($\Delta F/F_0$) at each CeO_2 concentration. At pH 4, the fluorescence initially dropped quickly.

With >20 μg mL^{-1} of CeO_2, however, little further quenching was observed (Figure 2b, green trace). Even with 500 μg mL^{-1} of CeO_2, quenching only reached ~30%. Therefore, the surface of DOPC liposomes was not fully occupied by CeO_2 at pH 4. CeO_2 NPs are positively charged at pH 4 (Figure 1C). The initially adsorbed CeO_2 may electrostatically repel further incoming NPs. To confirm this hypothesis, we then repeated the measurement in the presence of 150 mM NaCl to screen charge interactions (no NaCl was included in the previous experiment). In this case, we indeed observed stronger quenching reaching 50% (Figure 2b, red trace). This indicates that more CeO_2 NPs were adsorbed by screening the charge repulsion. The incomplete quenching can be explained by that only around 50% of the Rh-labels were on the outer leaflet of the bilayer, while the labels in the inner leaflet were not quenched by CeO_2. This also suggests that CeO_2 although small in size, did not penetrate through the bilayer membrane.

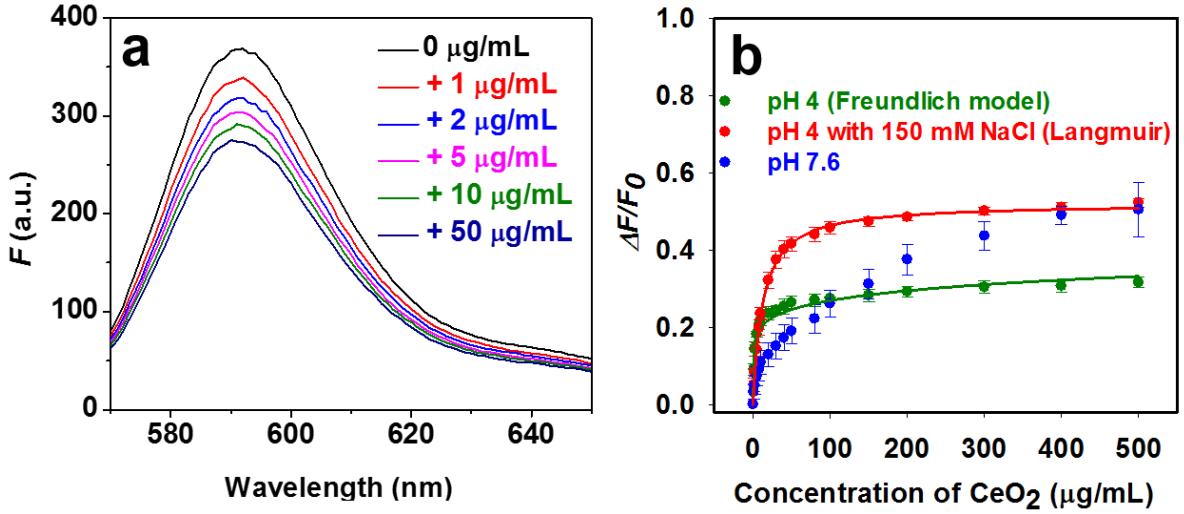

Figure 2. (a) Fluorescence spectra of the Rh-labeled DOPC liposomes at different CeO_2 concentrations dispersed in 25 mM acetate, pH 4. (b) Adsorption isotherms of CeO_2 NPs onto 50 μg mL^{-1} Rh-labeled DOPC liposomes at pH 4 without NaCl (green), with 150 mM NaCl (red), and at pH 7.6 without NaCl (blue).

The pH 4 plots in Figure 2b are essentially adsorption isotherms. For quantitative analysis, we fitted the data. At pH 4 without NaCl, a simple Langmuir isotherm failed to account for the data. The cationic CeO_2 NPs repel each other at pH 4, which conflicts with a basic assumption of Langmuir isotherm that adsorbed molecules do not interact. Thus, we fitted the data with the Freundlich isotherm $y=0.1478x^{0.13}$ (Figure 2b green trace), which takes into consideration lateral repulsion. On the other hand, adsorption at pH 4 with 150 mM NaCl was nicely fitted using the Langmuir isotherm model, because lateral electrostatic interactions were screened. Based on this fitting, a dissociation constant (K_d) of 12.4 μg mL^{-1} CeO_2 and a final quenching of 52% at full surface coverage are obtained.

On the other hand, at pH 7.6, the initial stage of quenching was milder, but the final quencher reached >50% (Figure 2b, blue trace). The UV-Vis spectra of both CeO_2 and its mixture with DOPC liposome showed a quite obvious light scattering effect due to aggregation of the involved particles (Figure S1b). As such, not all the decreased fluorescence is attributable to direct fluorescence quenching since light scattering can also contribute. Forming large aggregates is quite common in liposome/NP systems.[41-43] This complication made it difficult for quantitative data fitting, and the higher fluorescence drop beyond 50% at high CeO_2 concentrations might be a pure result of light scattering as the surface might have already been saturated. It is interesting to note that at pH 7.6, an initial high quenching efficiency was observed. At low CeO_2 concentrations, the light scattering effect is small, and this initial quenching is then supportive of CeO_2 adsorption. No fitting of this data set was performed due to the light scattering effect.

Lipid phosphate based adsorption. Since cerium is a hard metal that has a strong affinity to phosphate,[40, 44, 45] we propose that the phosphate group in the lipid might be playing a critical

role. To test this, we added free inorganic phosphate ions to the CeO_2 NPs prior to mixing them with DOPC (Figure 3a). In this case, free phosphate inhibited nanoceria adsorption at both pH 4 and 7.6. This supports the affinity between nanoceria and phosphate. Since adding phosphate has also increased the ionic strength of the solution, we also did a control experiment with 10-fold more NaCl added (Figure S2). In this case, efficient adsorption still occurred, confirming the specific role of phosphate. To further test this mechanism, we mixed DOPC and CeO_2 first, followed by adding phosphate to see if phosphate can displace CeO_2 (Figure 3b). Fluorescence was recovered at both pH's, indicating that the displacement reaction indeed occurred, also supporting CeO_2 interacting with phosphate group in the PC lipid.

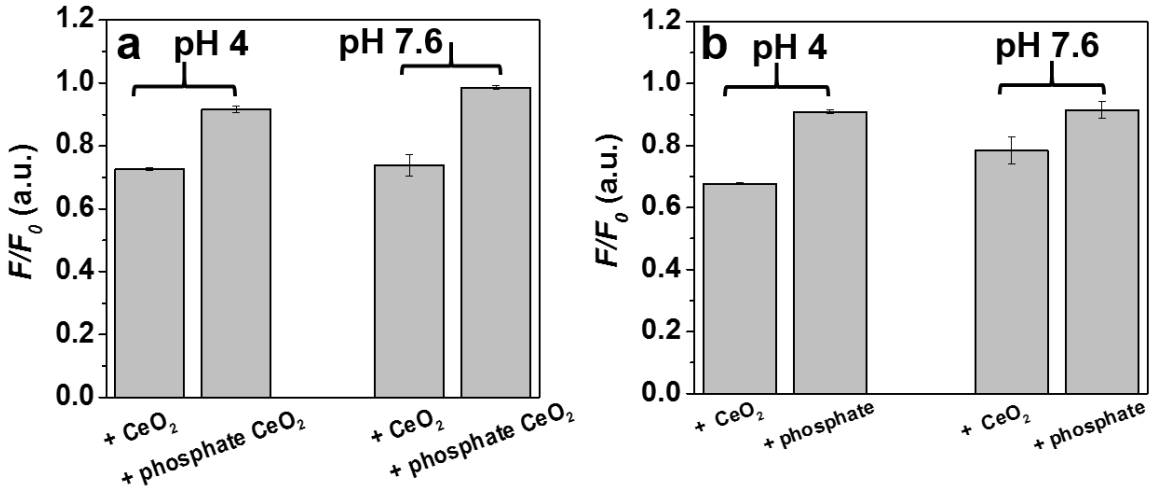

Figure 3. (a) Phosphate inhibited CeO_2 adsorption on the Rh-labeled DOPC liposomes (25 μg mL^{-1}) at pH 4 and pH 7.6. (b) Phosphate (10 mM) induced the CeO_2 desorption at pH 4 and pH 7.6.

Aggregation and re-stabilization of the adsorption complex. After confirming the adsorption of nanoceria by the liposomes, we next studied the further aggregation of this system. Since nanoceria may bridge a few liposomes, the system might grow into large aggregates. In this experiment, Rh-labeled liposomes were incubated with various concentrations of CeO_2. Then the mixture was centrifuged at 10,000 rpm for 10 min and the supernatant fluorescence intensity was measured. Free liposomes cannot be precipitated at this condition (Figure S3), allowing us to distinguish between well-dispersed liposomes and extensively aggregated structures. At pH 4, the supernatant fluorescence gradually decreased with increasing CeO_2 (Figure 4a, pink bars). The lowest fluorescence was achieved at a CeO_2 NPs concentration of 10 μg mL^{-1}. Under this condition, the precipitated liposome reached the maximal value. As the concentration of CeO_2 NPs was further increased, fluorescence started to increase again in the supernatant, suggesting liposome re-stabilization by CeO_2 NPs. This may be attributed to that at CeO_2 concentration lower than 10 μg mL^{-1}, the nanoparticles could bridge the liposomes to form aggregates with decreased stability. With more CeO_2 added, the bridging phenomenon was disrupted, and the whole liposome surface become positive charged due to the adsorption of CeO_2 NPs. Both contribute to the re-stabilization. At pH 7.6, however, no such re-stabilization was observed (Figure 4a, blue bars) since CeO_2 NPs are charge neutral at this pH, and there is no driving force for the bridges to be disrupted.

We also quantitatively measured the size and ζ-potential change when adding various amount of nanoceria to DOPC liposomes at pH 4 (Figure 4d-f). The size initially increased with the CeO_2 concentration up to 25 μg mL^{-1}, while further increase of CeO_2 has made the size smaller (Figure 4d). It is interesting to note that the largest size was still below 200 nm, suggesting that this system did not aggregate extensively at pH 4. With more than 100 μg mL^{-1}

of CeO_2, another peak just above 10 nm was observed, attributable to the free CeO_2 NPs (Figure 4e). The ζ-potential gradually increases with increasing CeO_2 concentration and reaches a plateau at 25 μg mL^{-1} (Figure 4f). This suggests that beyond this moment, all the measured surfaces were CeO_2, either as free NPs or adsorbed on the liposome.

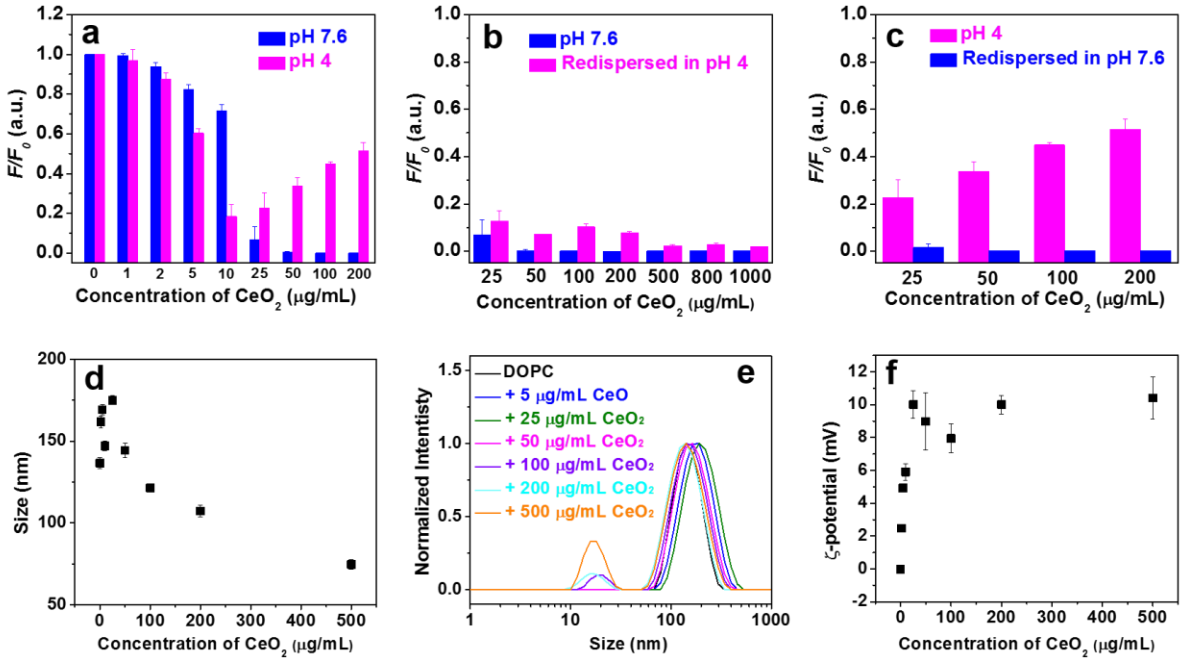

Figure 4. (a) Fluorescence of the supernatant after mixing CeO_2 and Rh-DOPC at pH 4 and pH 7.6 and then centrifugation. A finally increased fluorescence at pH 4 suggests re-stabilization of this system. (b) The complex prepared at pH 7.6 and re-dispersed at pH 4 failed to show re-stabilization. (c) The complex prepared at pH 4 and re-dispersed at pH 7.6. (d) Averaged hydrodynamic size of DOPC/CeO_2 complexes as a function of CeO_2 concentration at pH 4. (e) DLS spectra of DOPC/CeO_2 complexes with different CeO_2 amount at pH 4. (f) ζ-potential of DOPC/CeO_2 complexes as a function of CeO_2 concentration at pH 4.

In addition, when CeO_2 and DOPC were first mixed at pH 7.6 and then re-dispersed at pH 4, much less supernatant fluorescence was observed compared to those prepared at pH 4 directly (Figure 4b). This suggests that the majority of complexes formed at pH 7.6 were stably crosslinked by CeO_2 NPs. In comparison, when the CeO_2/DOPC complexes were prepared at pH 4 and re-dispersed at pH 7.6, no fluorescence was observed in the supernatant (Figure 4c). This indicates that the complexes were readily aggregated at pH 7.6, attributable to the lack of charge on the CeO_2 NPs at this pH.

Based on the above understanding, we proposed an interaction model. At pH 4, both the DOPC liposome and CeO_2 NPs are well dispersed in solution. At low CeO_2 concentrations, CeO_2 NPs moderately crosslink the liposomes, resulting in a small aggregates (<200 nm) that can be precipitate by centrifugation. With further increasing CeO_2 NPs, each liposome surface is densely covered by CeO_2 and the crosslinkers are disrupted, leading to re-stabilization (Scheme 1a). At pH 7.6, CeO_2 aggregation happened even in the absence of DOPC. Upon mixing, immediate crosslinking is formed by aggregated CeO_2 NPs and they remained aggregate even by adjusting the pH to 4 (Scheme 1b).

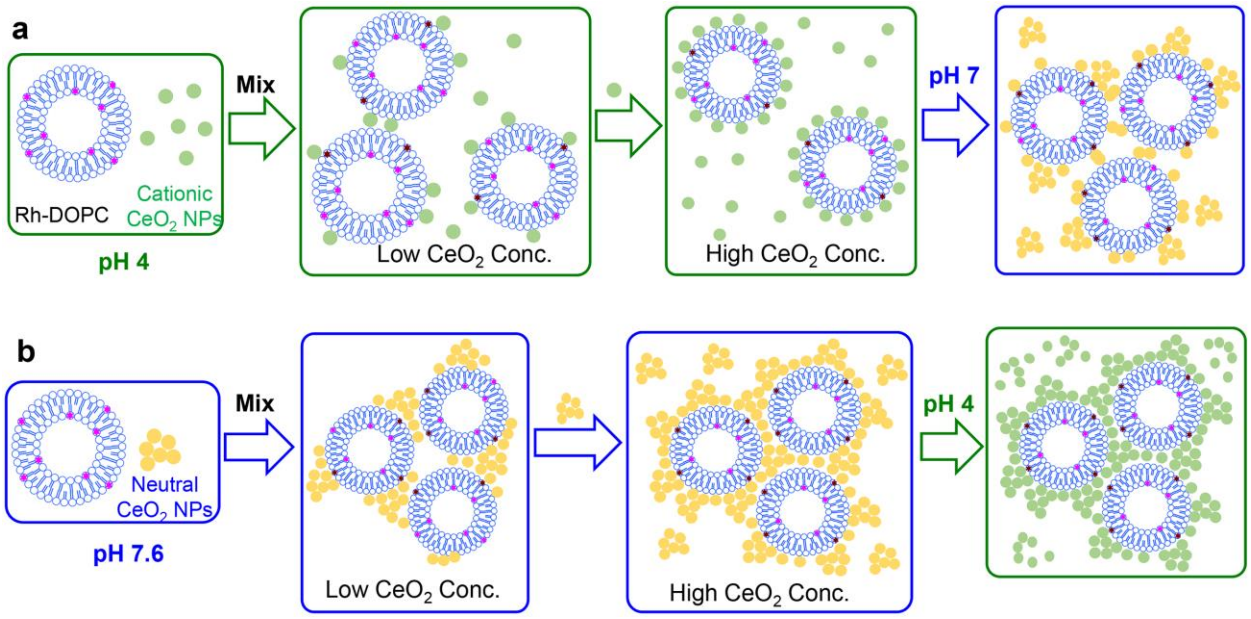

Scheme 1. Schematic illustration of adsorption of DOPC and CeO_2 at (a) pH 4 and (b) pH 7.6. At pH 4, there is a re-dispersion of the system by adding more CeO_2 NPs due to charge repulsion. At pH 7.6, CeO_2 NPs are nearly charge neutral, and are readily aggregated. The aggregates can further bridge liposomes to form even larger aggregates.

Nanoceria induces liposome leakage. A key question regarding nanoparticle/membrane interaction is membrane integrity, which can be probed by a leakage assay. In this work, ~100 mM calcein was encapsulated in each DOPC liposome and most of the free calcein molecules outside the liposome were removed. With such a high calcein concentration, its fluorescence is self-quenched. If the lipid membrane is disrupted, calcein is released into the whole solution yielding fluorescence enhancement. After mixing calcein-loaded liposomes with nanoceria, we observed an immediate fluorescence quenching, suggesting that nanoceria adsorbed the free calcein molecules outside the liposome (note that some free calcein still exists in our system). Adding Triton X-100 to fully rupture the membrane however still failed to induce fluorescence

enhancement and further quenching was observed (Figure 5a), which is also attributable to calcein adsorption by nanoceria. To confirm this, we added nanoceria to a free calcein solution and indeed we observed efficient fluorescence quenching (Figure 5b). Therefore, direct monitoring of fluorescence cannot be used here.

From our above studies, we know that nanoceria has a strong affinity to phosphate. We reason that phosphate might displace calcein from the nanoceria surface as schematically shown in Figure 5c. To confirm this, we added phosphate to the above control sample and indeed observed fluorescence increase (Figure 5b). With this in mind, we next added various concentrations of nanoceria to calcein-loaded DOPC liposomes at 5 min (Figure 5d). All the samples showed fluorescence quenching to the background level. At 25 min, we added phosphate and observed a strong fluorescence enhancement. With more CeO_2 added, higher fluorescence was observed after phosphate addition, and the recovered level was higher than the original level (e.g. fluorescence before 5 min). This indicates the liposome leaked upon addition of CeO_2 and the leaking process is CeO_2 concentration dependent. Further adding Triton-X100 fully ruptured liposomes and released all the encapsulated calcein.

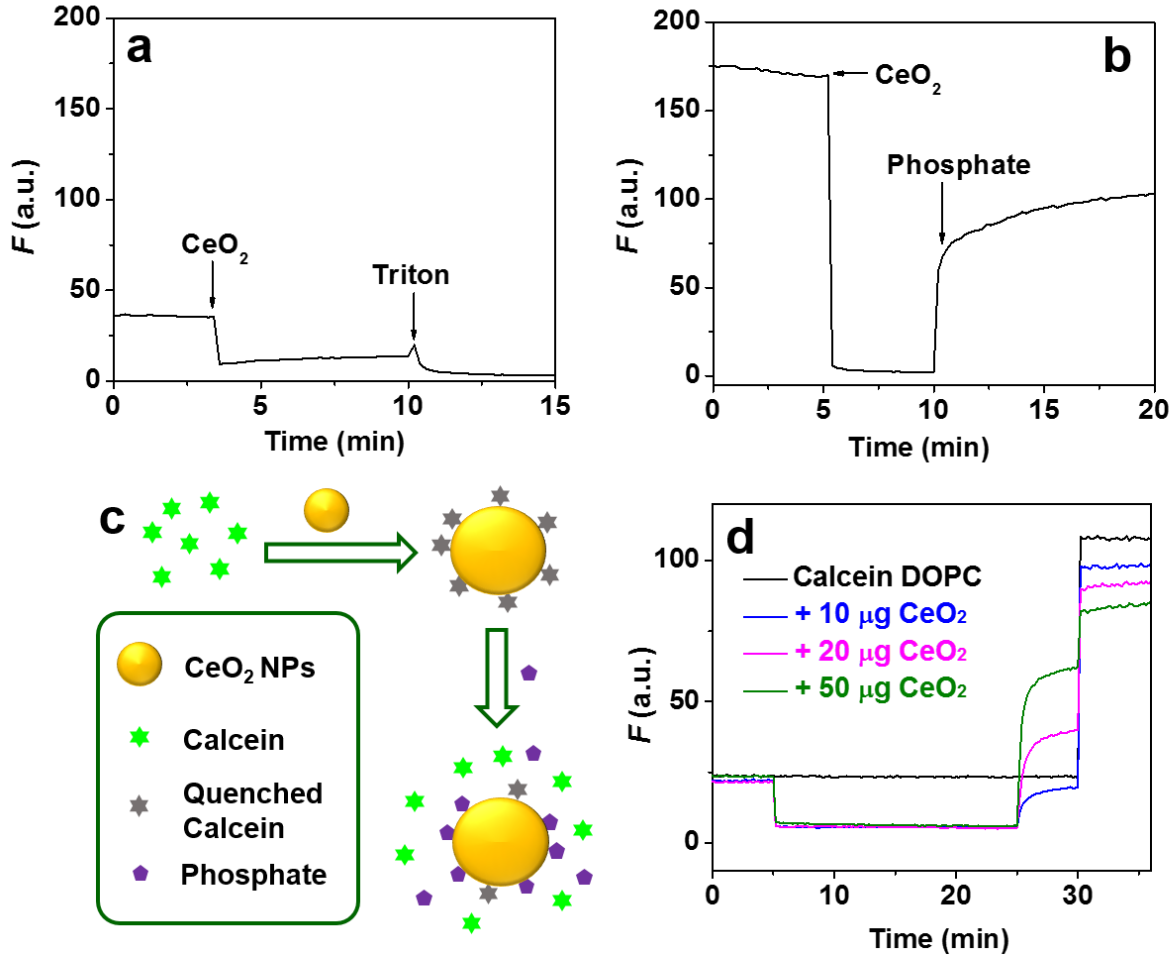

Figure 5. (a) Calcein-loaded DOPC leakage test by adding CeO_2 NPs. Triton X-100 was added to fully disrupt the liposomes. The quenching of fluorescence is due to calcein adsorption by CeO_2. (b) Phosphate displacement of free calcein adsorbed on CeO_2 NPs. (c) Schematic illustration of calcein fluorescence recovery by adding phosphate. (d) Leakage tests of calcein-loaded DOPC liposome by adding CeO_2 at 5 min. At 25 min, phosphate was added, and at 30 min, Triton X-100 was added.

Cryo-TEM characterization. This is the first time that we observed DOPC liposome leakage when mixed with a non-silica and non-cationic oxide.[46] At pH 7.6, CeO_2 is near charge neutral (slightly negatively charged), and thus the leakage is unlikely due to membrane damage by cationic nanomaterials.[46, 47] From the surface chemistry standpoint, CeO_2 is more similar to TiO_2 in terms of containing a hard Lewis acid metal favoring strong phosphate interaction, which is demonstrated in this work. Therefore, we want to understand whether this is due to fully ruptured liposomes or local membrane damages. For this purpose, TEM was used. Using the normal TEM, we observed that the distribution of CeO_2 (Figure 6a) is quite different from that in the absence and presence of liposome (inset of Figure 1a). While we can see the CeO_2 NPs distributed around a liposome shaped contour, we cannot resolve the liposomes. Using cryo-TEM, we indeed observed CeO_2 adsorption and the liposome structure was still largely maintained, although deformation of liposomes from perfect spherical structure was also observed (Figure 6b).

As such, the leakage must be due to local interaction between CeO_2 and the liposomes. As a further control, we tested calcein-loaded DPPC liposomes, and CeO_2 NPs failed to leak them (Figure 6c). DPPC and DOPC have the same headgroup chemistry, and the only difference is that DPPC is in the gel phase at room temperature with a phase transition temperature (T_c) of 41 °C. On the other hand, DOPC has a T_c of -20 °C and is fluid at room temperature. Therefore, leakage of DOPC liposomes is likely to relate to the T_c.

One possibility is that the adsorption is very strong, and it can raise the T_c of the lipid at the spot of adsorption.[22] We observed such a phenomenon with gold nanoparticles.[43, 48] In that case, we attributed it to the strong van der Waals force between gold and liposome. Here, the CeO_2 NPs were brought very close to the liposome surface by the lipid phosphate interaction. If

this hypothesis is true, CeO_2 NPs should increase the T_c of liposomes. Therefore, we used DSC to measure the DPPC liposomes (Figure 6d). Free DPPC has a T_c of 41 °C as expected. After adding a 1:1 mass ratio of CeO_2 NPs, its T_c shifted to 42.5 °C. Further increase the CeO_2 concentration by 5-fold raised the T_c to 43.2 °C with a significant peak broadening. We reason that at the spot of adsorption, the DOPC lipids underwent a fluid-to-gel phase transition, and calcein can leak during this transition period. Once adsorbed, the liposome becomes stable again. [22, 43, 48, 49] The DPPC liposome is already in the gel phase, and thus adding nanoceria would not induce the phase transition and thus no leakage took place.

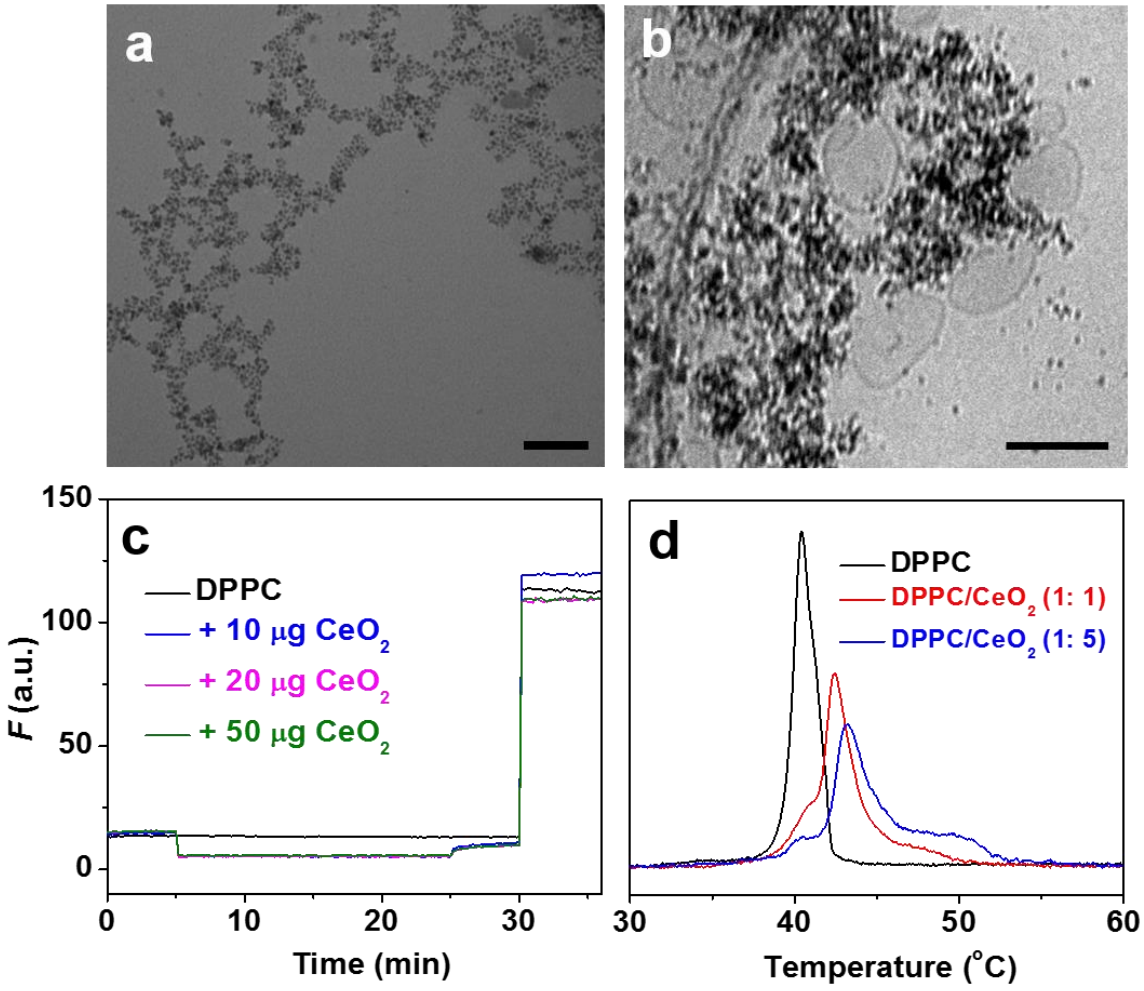

Figure 6. TEM image (a) and Cryo-TEM (b) of DOPC liposome mixed with CeO_2 NPs (scale bars = 100 nm). (c) Calcein leakage tests of DPPC liposomes with CeO_2 added at 5 min, phosphate added at 25 min and Triton X-100 added at 30 min. The buffer was 25 mM HEPES (pH 7.6). The final fluorescence after adding phosphate was lower than the initial fluorescence regardless of CeO_2 concentration, suggesting no leakage occurred. (d) DCS traces of DPPC liposomes as a function of CeO_2 concentration. The ratio refers to the mass concentration of DPPC and CeO_2.

While this is a model study performed in a reduced physical system, it still has interesting biological implications. For example, nanoceria alone cannot enter the membrane and it has to be internalized by cells by active transportation, likely via endocytosis.[10, 16] In the acidic endosome and lysosome, the surface charge of nanoceria changes from neutral to positive, and this is likely to have an influence on its membrane interactions. Nanoceria can strongly bind to the phosphate group in lipids and this is likely to be true for all the phospholipids. Such interaction can even change the lipid phase transition temperature and induce a transient membrane leakage.

Conclusions

In summary, the interaction between PC liposomes and CeO_2 NPs were systematically studied using a suite of techniques. We are interested in nanoceria due to its anti-oxidation activity widely tested in many cellular and animal studies in recent years. Two types of liposomes: DOPC and DPPC were included in this study. They have the same headgroup chemistry but different T_c. The fluorescence quenching experiments indicated that CeO_2 NPs are adsorbed by

DOPC at both pH 4 and pH 7.6. The interaction between the phosphate in the lipid headgroup and CeO_2 is mainly responsible for the adsorption. At pH 4, CeO_2 NPs are positively charged, while at pH 7.6, they are nearly charge neutral. Such electrostatic factors showed a strong influence on the observed adsorption isotherms. When CeO_2 is positively charged, the complexes can be re-stabilized with relatively higher amount of CeO_2 NPs. CeO_2 could induce the leakage of DOPC. This is the first time that we observed that DOPC liposome leaked by a non-cationic metal oxide, and the leakage was attributed the CeO_2 adsorption induced local fluid-to-gel phase transition. This work provides fundamental understandings of the interaction between lipid bilayers and CeO_2 NPs at the molecular level, which may offer insights into CeO_2 interaction with cell membranes.

ASSOCIATED CONTENT

Supporting Information

The Supporting Information is available free of charge on the ACS Publications website at DOI:

UV-Vis spectra of CeO_2 and CeO_2/DOPC complexes at pH 4 and pH 7.6 (Figure S1), fluorescence adsorption of Rh-DOPC with the addition of CeO_2 and NaCl (Figure S2) and fluorescence spectra of Rh-DOPC before and after centrifugation at pH 7.6 and pH 4 (Figure S3)**.**

Author Information

Corresponding Author

* Email: liujw@uwaterloo.ca.

Notes

The authors declare no competing financial interest.

Acknowledgement

We thank Robert Harris at the University of Guelph for assistance during the cryo-TEM experiment and Biwu Liu for HRTEM. Funding for this work is from the Natural Sciences and Engineering Research Council of Canada (NSERC).

References

(1) Montini, T.; Melchionna, M.; Monai, M.; Fornasiero, P., Fundamentals and Catalytic Applications of CeO_2-Based Materials. *Chem. Rev.* **2016**, 116, 5987-6041.

(2) Xu, C.; Qu, X., Cerium Oxide Nanoparticle: A Remarkably Versatile Rare Earth Nanomaterial for Biological Applications. *NPG Asia Mater* **2014**, 6, e90.

(3) Ujjain, S. K.; Das, A.; Srivastava, G.; Ahuja, P.; Roy, M.; Arya, A.; Bhargava, K.; Sethy, N.; Singh, S. K.; Sharma, R. K.; Das, M., Nanoceria Based Electrochemical Sensor for Hydrogen Peroxide Detection. *Biointerphases* **2014**, 9, 031011.

(4) Celardo, I.; Pedersen, J. Z.; Traversa, E.; Ghibelli, L., Pharmacological Potential of Cerium Oxide Nanoparticles. *Nanoscale* **2011**, 3, 1411-1420.

(5) Korsvik, C.; Patil, S.; Seal, S.; Self, W. T., Superoxide Dismutase Mimetic Properties Exhibited by Vacancy Engineered Ceria Nanoparticles. *Chem. Commun.* **2007**, 1056-1058.

(6) Dowding, J. M.; Das, S.; Kumar, A.; Dosani, T.; McCormack, R.; Gupta, A.; Sayle, T. X. T.; Sayle, D. C.; von Kalm, L.; Seal, S.; Self, W. T., Cellular Interaction and Toxicity Depend on Physicochemical Properties and Surface Modification of Redox-Active Nanomaterials. *ACS Nano* **2013**, 7, 4855-4868.

(7) Chen, J.; Patil, S.; Seal, S.; McGinnis, J. F., Rare Earth Nanoparticles Prevent Retinal Degeneration Induced by Intracellular Peroxides. *Nat Nano* **2006**, 1, 142-150.

(8) Lin, Y. H.; Ren, J. S.; Qu, X. G., Catalytically Active Nanomaterials: A Promising Candidate for Artificial Enzymes. *Acc. Chem. Res.* **2014**, 47, 1097-1105.

(9) Walkey, C.; Das, S.; Seal, S.; Erlichman, J.; Heckman, K.; Ghibelli, L.; Traversa, E.; McGinnis, J. F.; Self, W. T., Catalytic Properties and Biomedical Applications of Cerium Oxide Nanoparticles. *Environ. Sci. Nano* **2015**, 2, 33-53.

(10) Xia, T.; Kovochich, M.; Liong, M.; Mädler, L.; Gilbert, B.; Shi, H.; Yeh, J. I.; Zink, J. I.; Nel, A. E., Comparison of the Mechanism of Toxicity of Zinc Oxide and Cerium Oxide Nanoparticles Based on Dissolution and Oxidative Stress Properties. *ACS Nano* **2008**, 2, 2121-2134.

(11) Hirst, S. M.; Karakoti, A. S.; Tyler, R. D.; Sriranganathan, N.; Seal, S.; Reilly, C. M., Anti-Inflammatory Properties of Cerium Oxide Nanoparticles. *Small* **2009**, 5, 2848-2856.

(12) Lyu, G.-M.; Wang, Y.-J.; Huang, X.; Zhang, H.-Y.; Sun, L.-D.; Liu, Y.-J.; Yan, C.-H., Hydrophilic CeO_2 Nanocubes Protect Pancreatic β-Cell Line Ins-1 from H_2O_2-Induced Oxidative Stress. *Nanoscale* **2016**, 8, 7923-7932.

(13) Celardo, I.; De Nicola, M.; Mandoli, C.; Pedersen, J. Z.; Traversa, E.; Ghibelli, L., Ce^{3+} Ions Determine Redox-Dependent Anti-Apoptotic Effect of Cerium Oxide Nanoparticles. *ACS Nano* **2011**, 5, 4537-4549.

(14) Perez, J. M.; Asati, A.; Nath, S.; Kaittanis, C., Synthesis of Biocompatible Dextran-Coated Nanoceria with pH-Dependent Antioxidant Properties. *Small* **2008**, 4, 552-556.

(15) Tarnuzzer, R. W.; Colon, J.; Patil, S.; Seal, S., Vacancy Engineered Ceria Nanostructures for Protection from Radiation-Induced Cellular Damage. *Nano Lett.* **2005**, 5, 2573-2577.

(16) Ji, Z.; Wang, X.; Zhang, H.; Lin, S.; Meng, H.; Sun, B.; George, S.; Xia, T.; Nel, A. E.; Zink, J. I., Designed Synthesis of CeO_2 Nanorods and Nanowires for Studying Toxicological Effects of High Aspect Ratio Nanomaterials. *ACS Nano* **2012**, 6, 5366-5380.

(17) Kim, C. K.; Kim, T.; Choi, I.-Y.; Soh, M.; Kim, D.; Kim, Y.-J.; Jang, H.; Yang, H.-S.; Kim, J. Y.; Park, H.-K.; Park, S. P.; Park, S.; Yu, T.; Yoon, B.-W.; Lee, S.-H.; Hyeon, T., Ceria Nanoparticles That Can Protect against Ischemic Stroke. *Angew. Chem., Int. Ed.* **2012**, 51, 11039-11043.

(18) Kumar, A.; Das, S.; Munusamy, P.; Self, W.; Baer, D. R.; Sayle, D. C.; Seal, S., Behavior of Nanoceria in Biologically-Relevant Environments. *Environ. Sci. Nano* **2014**, 1, 516-532.

(19) Nel, A. E.; Madler, L.; Velegol, D.; Xia, T.; Hoek, E. M. V.; Somasundaran, P.; Klaessig, F.; Castranova, V.; Thompson, M., Understanding Biophysicochemical Interactions at the Nano-Bio Interface. *Nat. Mater.* **2009**, 8, 543-557.

(20) Verma, A.; Stellacci, F., Effect of Surface Properties on Nanoparticle-Cell Interactions. *Small* **2010**, 6, 12-21.

(21) Liu, J., Interfacing Zwitterionic Liposomes with Inorganic Nanomaterials: Surface Forces, Membrane Integrity, and Applications. *Langmuir* **2016**, 32, 4393-4404.

(22) Wang, B.; Zhang, L. F.; Bae, S. C.; Granick, S., Nanoparticle-Induced Surface Reconstruction of Phospholipid Membranes. *Proc. Natl. Acad. Sci. U.S.A.* **2008**, 105, 18171-18175.

(23) Gao, W.; Hu, C.-M. J.; Fang, R. H.; Zhang, L., Liposome-Like Nanostructures for Drug Delivery. *J. Mater. Chem. B* **2013**, 1, 6569-6585.

(24) Tan, S.; Li, X.; Guo, Y.; Zhang, Z., Lipid-Enveloped Hybrid Nanoparticles for Drug Delivery. *Nanoscale* **2012**, 5, 860-872.

(25) Rascol, E.; Devoisselle, J.-M.; Chopineau, J., The Relevance of Membrane Models to Understand Nanoparticles-Cell Membrane Interactions. *Nanoscale* **2016**, 8, 4780-4798.

(26) Oliver, A. E.; Parikh, A. N., Templating Membrane Assembly, Structure, and Dynamics Using Engineered Interfaces. *Biochimica Et Biophysica Acta-Biomembranes* **2010**, 1798, 839-850.

(27) Wang, F.; Liu, J., Liposome Supported Metal Oxide Nanoparticles: Interaction Mechanism, Light Controlled Content Release, and Intracellular Delivery. *Small* **2014**, 10, 3927-3931.

(28) Wang, F.; Liu, J., A Stable Lipid/TiO_2 Interface with Headgroup-Inversed Phosphocholine and a Comparison with SiO_2. *J. Am. Chem. Soc.* **2015**, 137, 11736-11742.

(29) Reimhult, E.; Hook, F.; Kasemo, B., Intact Vesicle Adsorption and Supported Biomembrane Formation from Vesicles in Solution: Influence of Surface Chemistry, Vesicle Size, Temperature, and Osmotic Pressure *Langmuir* **2003**, 19, 1681-1691.

(30) Ip, A. C. F.; Liu, B.; Huang, P.-J. J.; Liu, J., Oxidation Level-Dependent Zwitterionic Liposome Adsorption and Rupture by Graphene-Based Materials and Light-Induced Content Release. *Small* **2013**, 9, 1030-1035.

(31) Cremer, P. S.; Boxer, S. G., Formation and Spreading of Lipid Bilayers on Planar Glass Supports. *J. Phys. Chem. B* **1999**, 103, 2554-2559.

(32) Mornet, S.; Lambert, O.; Duguet, E.; Brisson, A., The Formation of Supported Lipid Bilayers on Silica Nanoparticles Revealed by Cryoelectron Microscopy. *Nano Lett.* **2005**, 5, 281-285.

(33) Richter, R. P.; Berat, R.; Brisson, A. R., Formation of Solid-Supported Lipid Bilayers: An Integrated View. *Langmuir* **2006**, 22, 3497-3505.

(34) Cho, N.-J.; Jackman, J. A.; Liu, M.; Frank, C. W., pH-Driven Assembly of Various Supported Lipid Platforms: A Comparative Study on Silicon Oxide and Titanium Oxide. *Langmuir* **2011**, 27, 3739-3748.

(35) Jackman, J. A.; Zan, G. H.; Zhao, Z.; Cho, N.-J., Contribution of the Hydration Force to Vesicle Adhesion on Titanium Oxide. *Langmuir* **2014**, 30, 5368-5372.

(36) Michel, R.; Kesselman, E.; Plostica, T.; Danino, D.; Gradzielski, M., Internalization of Silica Nanoparticles into Fluid Liposomes: Formation of Interesting Hybrid Colloids. *Angew. Chem. Int. Ed.* **2014**, 53, 12441-12445.

(37) Sehgal, A.; Lalatonne, Y.; Berret, J. F.; Morvan, M., Precipitation−Redispersion of Cerium Oxide Nanoparticles with Poly(Acrylic Acid): Toward Stable Dispersions. *Langmuir* **2005**, 21, 9359-9364.

(38) Qi, L.; Sehgal, A.; Castaing, J.-C.; Chapel, J.-P.; Fresnais, J. r. m.; Berret, J.-F. o.; Cousin, F., Redispersible Hybrid Nanopowders: Cerium Oxide Nanoparticle Complexes with Phosphonated-Peg Oligomers. *ACS Nano* **2008**, 2, 879-888.

(39) Asati, A.; Santra, S.; Kaittanis, C.; Nath, S.; Perez, J. M., Oxidase-Like Activity of Polymer-Coated Cerium Oxide Nanoparticles. *Angew. Chem., Int. Ed.* **2009**, 48, 2308-2312.

(40) Pautler, R.; Kelly, E. Y.; Huang, P.-J. J.; Cao, J.; Liu, B.; Liu, J., Attaching DNA to Nanoceria: Regulating Oxidase Activity and Fluorescence Quenching. *ACS Appl. Mater. Inter*. **2013**, 5, 6820–6825.

(41) Mousseau, F.; Le Borgne, R.; Seyrek, E.; Berret, J. F., Biophysicochemical Interaction of a Clinical Pulmonary Surfactant with Nanoalumina. *Langmuir* **2015**, 31, 7346-7354.

(42) Wang, F.; Liu, J., Nanodiamond Decorated Liposomes as Highly Biocompatible Delivery Vehicles and a Comparison with Carbon Nanotubes and Graphene Oxide. *Nanoscale* **2013**, 5, 12375-12382.

(43) Wang, F.; Curry, D. E.; Liu, J., Driving Adsorbed Gold Nanoparticle Assembly by Merging Lipid Gel/Fluid Interfaces. *Langmuir* **2015**, 31, 13271-13274.

(44) McCormack, R. N.; Mendez, P.; Barkam, S.; Neal, C. J.; Das, S.; Seal, S., Inhibition of Nanoceria's Catalytic Activity Due to Ce^{3+} Site-Specific Interaction with Phosphate Ions. *J. Phys. Chem. C* **2014**, 118, 18992-19006.

(45) Liu, B.; Sun, Z.; Huang, P.-J. J.; Liu, J., Hydrogen Peroxide Displacing DNA from Nanoceria: Mechanism and Detection of Glucose in Serum. *J. Am. Chem. Soc.* **2015**, 137, 1290-1295.

(46) Wang, F.; Zhang, X.; Liu, Y.; Lin, Z. Y.; Liu, B.; Liu, J., Profiling Metal Oxides with Lipids: Magnetic Liposomal Nanoparticles Displaying DNA and Proteins. *Angew. Chem., Int. Ed.* **2016**, 55, 12063–12067.

(47) Leroueil, P. R.; Berry, S. A.; Duthie, K.; Han, G.; Rotello, V. M.; McNerny, D. Q.; Baker, J. R.; Orr, B. G.; Banaszak Holl, M. B., Wide Varieties of Cationic Nanoparticles Induce Defects in Supported Lipid Bilayers. *Nano Lett.* **2008**, 8, 420-424.

(48) Wang, F.; Liu, J., Self-Healable and Reversible Liposome Leakage by Citrate-Capped Gold Nanoparticles: Probing the Initial Adsorption/Desorption Induced Lipid Phase Transition. *Nanoscale* **2015**, 7, 15599-15604.

(49) Zhang, L. F.; Granick, S., How to Stabilize Phospholipid Liposomes (Using Nanoparticles). *Nano Lett.* **2006**, 6, 694-698.